



PROFESSOR CHANGSONG XU (Orcid ID : 0000-0003-3843-5096)

Article type : Research Article

Design and development of novel thiazolidin-4-one-1,3,5-triazine derivatives as neuro-protective agent against cerebral ischemia reperfusion injury in mice *via* attenuation of NF- κ B

Min Lu¹, Yujun Qi¹, Yu Han¹, Qiong Yi¹, Lei Xu¹, Wenlin Sun¹, Guihua Ni², Xiaoyu Ni¹, Changsong Xu^{2*}

¹Department of Rehabilitation Medicine, The Affiliated Huai'an No.1 People's Hospital of Nanjing Medical University, Huai'an, Jiangsu 223300, P.R. China

²Department of Neurology, The Affiliated Huai'an No.1 People's Hospital of Nanjing Medical University, Huai'an, Jiangsu 223300, P.R. China

Short running title: Thiazolidin-4-one-1,3,5-triazine as neuro-protective agent

This article has been accepted for publication and undergone full peer review but has not been through the copyediting, typesetting, pagination and proofreading process, which may lead to differences between this version and the [Version of Record](#). Please cite this article as [doi: 10.1111/CBDD.13744](https://doi.org/10.1111/CBDD.13744)

This article is protected by copyright. All rights reserved

***Corresponding Author:**

Changsong Xu,

Department of Neurology, The Affiliated Huai'an No.1 people's Hospital of Nanjing Medical University, Huai'an, Jiangsu 223300, P.R. China

Tel/fax: +86 517 8495 9789

Email: coleridgerwqbvds@gmail.com

Abstract

The present study enumerates the discovery and development of novel thiazolidin-4-one-1,3,5-triazine as neuro-protective agent against cerebral ischemia reperfusion injury in mice. These compounds showed significant inhibition of NF- κ B transcriptional activity in LPS-stimulated RAW264.7 cells, displaying compound **8k** as most potent inhibitor among the tested derivative. The compound **8k** was further studied in *in-vivo* middle cerebral artery occlusion (MCAO) mice model for neuro-protective action. Results suggest that compound **8k** causes attenuation of inflammation (TNF- α , IL- β and IL-6), oxidative stress (SOD, GSH and MDA) and apoptosis (Bcl-2, Bax and cleaved caspase-3) in MCAO mice in concentration dependent manner. Collectively,

our results documented that compound **8k** pre-treatment protects cerebral I/R. This novel lead scaffold may be helpful for investigation of new neuro-protective agent by inactivation of NF- κ B.

Keywords: Thiazolidin-4-one; 1,3,5-triazine; MCAO; NF- κ B; inflammation; oxidative stress.

1. Introduction

The increased life expectancy has concomitantly raise chances of cerebrovascular disease (CVD), where the blood flow to/in the brain is temporarily or permanently blocked. It is a serious debilitating condition responsible for long-term disability and one of the three most prominent cause of death worldwide (Avery et al., 2016; Truelsen et al., 2000). Cerebral ischemic stroke is one of the major causes of CVD where, an artery to the brain is blocked. It reduces the blood flow and oxygen to the brain, leading to damage or death of brain cells. However, after restoration of blood flow it may induce cerebral ischemia and reperfusion (I/R) injury due to generation of various reactive oxygen species (ROS), inflammatory cytokines and pro-inflammatory mediators which worsen neuronal injury and induces neuronal apoptosis (Astrup et al., 1981; Broughton et

al., 2009; Jin et al., 2010; Huang et al., 2006). Therefore, many researchers across the world are currently involved in development of novel anti-inflammatory agents which can be able to inhibit inflammatory cascade involved in cerebral I/R injury (Lakhan et al., 2009).

Nuclear factor κ B (NF- κ B), a member of transcription factors family recognized to transform variety of metabolic events including cell survival, inflammation, apoptosis and even autophagic cell death (Zhang et al., 2017; Hayden & Ghosh, 2004). The patients of cerebral I/R injury showed aberrant activation of NF- κ B which mediate cascade of inflammatory response upon activation by any external stimuli, such as, cytokines (interleukins), bacterial products (LPS) and oxidative stress (Ridder & Schwaninger 2009; Zhang et al., 2005). It was suggests being involved in gene transcription after translocation to nucleus and induces expression of interleukin-1 (IL-1), IL-6, tumor necrosis factor- α (TNF- α), and resulted in neuronal death (Karin & Ben-Neriah, 2000; Shih et al., 2015). Thus, various studies showed NF- κ B inhibitors have beneficial role against cerebral I/R injury.

Thiazolidin-4-one is a heterocyclic molecule well-known for excellent pharmacological activities, for instance, anti-bacterial (Vicini et al., 2006; Dwivedi et al., 2016), anti-cancer (Joseph et al., 2013; Rashid et al., 2014), anti-viral (Murugesan et al., 2014) and anti-inflammatory (Vazzana et al., 2004). On the contrary, 1,3,5-triazine is also a versatile lead molecule exhibiting numerous biological activities, including antibacterial (Singh et al., 2014; Singh et al., 2012), antifungal (Singh et al., 2012; Singh, et al., 2013; Vembu et al., 2016), anticancer (Popowycz et al., 2009; Hodous et al., 2007; Dao et al., 2015) and more importantly anti-inflammatory action (Mogilski et al., 2017; Zacharie et al., 2018). Moreover, the pioneering study by Shrivastava et al. reported a series of thiazolidin-4-one-1,3,5-triazine as potent NF- κ B inhibitor for airway inflammation in cystic fibrosis (Srivastava et al., 2015). Prompted by the above, in present study, we wish to develop hybrid conjugates of thiazolidin-4-one-1,3,5-triazine in search of potent anti-inflammatory agent against cerebral I/R injury.

2. Result and Discussion

2.1. *Synthesis of hybrid conjugates of thiazolidin-4-one-1,3,5-triazine*

The compounds were synthesized using facile route as outlined in Scheme 1 in excellent yields. Briefly, the synthesis was initiated by nucleophilic reaction between 2,4,6-tri chloro-1,3,5-triazine (**1**) with substituted anilines **2(a-g)** to furnish compounds **3(a-g)**. The morpholine was

reacted with compounds **3(a-g)** to afford compound **4(a-g)**. In the next step, aqueous ammonia was used to liberate remaining chlorine atom to yield compounds **5(a-g)**. The last step corresponds to the one-pot synthesis of targeted derivatives **8(a-n)** by refluxing together compounds **5(a-g)**, substituted aldehydes **6(a-b)** and mercaptoacetic acid (**7**).

<Scheme 1>

2.2. *In vitro* NF- κ B transcription inhibitory activity

In the present study, we have developed hybrid molecules of thiazolidin-4-one and 1,3,5-triazine in a search of better NF- κ B inhibitor against cerebral I/R injury. The present strategy is aimed to enhance the pharmacological spectrum of the hybrid derivatives by taking the advantage of two different skeletons which might act in synergistic manner than individual component. The multifactorial etiology of cerebral I/R injury is suitable towards this approach and might provide additional benefit. The NF- κ B is a dimeric protein corresponds to a family of transcription factors (Rel/NF- κ B) which bound to specific I κ B in cytoplasm in dormant state and upon activation it translocates to nucleus where it bind to target genes and control transcription of numerous genes. The experimental and clinical evidences have confirmed oxidative stress in the cerebral I/R injury triggers the activation of NF- κ B signaling pathway which induces neuronal inflammation (Conner & Grisham, 1996; Lordan et al., 2019; Halliwell, 2006). Thus, inhibition of NF- κ B activation provides significant benefit against neuronal inflammation in cerebral I/R injury. As presented in table 1, the synthesized hybrid conjugates of pyrazole-1,3,5-triazine (**8a-n**) were tested for inhibitory effect on NF- κ B transcriptional activity in LPS-stimulated RAW264.7 cells. The two different set of molecules were developed by taking *para*-chloro (**8a-g**) and *para*-fluro (**8h-n**) atoms on the phenyl of thiazolidin-4-one using different substitutions on the phenyl linked to 1,3,5-triazine core. The compound **8a** containing un-substituted phenyl connected to 1,3,5-triazine core along with *para*-chloro on the phenyl ring connected to thiazolidin-4-one scaffold showed least effect on NF- κ B transcriptional activity in LPS-stimulated RAW264.7 cells. However, introduction of *para*-chloro at the un-substituted phenyl ring (**8b**) displayed drastic improvement in inhibitory potency. The inhibitory potency was further improved significantly in the case of compounds **8c** ($IC_{50} = 19.23 \pm 2.11$) and **8d** ($IC_{50} = 15.65 \pm 1.92$) containing *para*-fluro and *para*-nitro atoms, respectively. To our surprise, the activity was significantly reduced on introduction of *para*-hydroxy ($IC_{50} = 31.36 \pm 3.72$) and *para*-methoxy ($IC_{50} = 49.56 \pm 4.73$) in the case of

compounds **8e** and **8f**, correspondingly. The last compound of this set (**8g**) showed least potent activity among the developed compounds of both the series. On closely inspecting table 1, the inhibitory activity was found increased in next set of compounds containing *para*-fluro (**8h-n**) on the phenyl of thiazolidin-4-one as compared to *para*-chloro (**8a-g**) counterparts. The compound **8h** displayed moderate inhibitory activity on NF- κ B transcriptional activity. The inhibitory activity was significantly improved in the case of compound **8i** with *para*-chloro substitution ($IC_{50} = 3.33 \pm 0.23$). On replacement of *para*-chloro with *para*-fluoro (**8j**), the activity was slightly reduced. However, introduction of *para*-nitro ($IC_{50} = 0.90 \pm 0.12$) render compound most potent among the tested derivatives, even more potent that reference compound. The activity was found reduced in the case of compounds **8l** ($IC_{50} = 5.89 \pm 1.14$), **8m** ($IC_{50} = 10.11 \pm 2.33$) and **8n** ($IC_{50} = 7.34 \pm 1.50$) against NF- κ B transcriptional activity in LPS-stimulated RAW264.7 cells. In the present study, the control group was deemed as RAW264.7 cells without stimulated by LPS, while LPS group was considered as stimulated RAW264.7 cells by LPS without any treatment. Dexamethasones serve as reference compound in the present study. Based on the comparative inhibitory potency of compounds **8a-n** against NF- κ B transcriptional activity in LPS-stimulated RAW264.7 cells, the structure-activity relationship (SAR) suggest that, the pattern of substitution have strong influence on the pharmacological activity. The results corroborated that the compounds containing *para*-fluro on the thiazolidin-4-one scaffold proved much efficient than their *para*-chloro counterparts. The detailed analysis of activity chart further revealed that, un-substitution is not favourable for inhibitory activity, while introduction of substitution render compound more active. It was also marked to note that, more pronounced activity was revealed by electron withdrawing group than their electron-donating counterpart, and the order of activity is as follows $NO_2 > Cl > F > OH > OCH_3 > CH_3 > H$.

<Table 1>

2.3. *In vivo* pharmacological activity

Impressed by the excellent NF- κ B transcription inhibitory activity, it is worthwhile to analyze the effect of most potent NF- κ B inhibitor compound **8k** in the experimentally induced cerebral I/R injury by middle cerebral artery embolism (MCAO) in mice (McCullough et al., 2011; Chiang et al., 2011). Various clinical studies have shown impairment of neural function and cerebral edema is the characteristic hallmark of cerebral injury (Werner & Engelhard, 2007; Unterberg et al.,

2004). Therefore, initially after induction of cerebral I/R injury by MCAO, the effect of compound **8k** was investigated on the neural function and cerebral edema in the brains of mice. As shown in Fig.1A, the neurological deficit score of compound **8k** treated group which signifies the neural function of brain was found to be improved as compared to MCAO-treatment group in dose dependent manner ($P > 0.05$). In the next instance, as shown in Fig. 1B, the MCAO treated mice demonstrated increased cerebral edema as compared to sham. However, the cerebral edema was found to be reduced significantly in compound **8k** treated mice.

<Figure 1>

The effect of compound **8k** was further studied visually by examining the histopathological changes in MCAO-treated mice brains. It provides idea about clinical manifestation of disease and the effect of drugs/treatment on the affected tissues *via* microscopic means. As shown in Fig. 2, the MCAO treated mice showed reduced nerve cells, disordered arrangement of cells and enhanced intracellular spaces, as compared to sham, which had not any such features. Whereas, in **8k** treated mice, these features were found to be returned to near normal in concentration dependent manner.

<Figure 2>

Infarction is the main consequence of ischemia of brain in cerebral injury, whereas, restoration of normal brain function after reperfusion will be entirely dependent on the area of non-infracted tissues (Chan, 2001). Therefore, many therapeutic modalities to treat cerebral injury are majorly concentrated towards prompt reperfusion and drugs to prevent infarction. In this regard, our next aim to determine the effect of compound **8k** on the brain infarct size to assess its protective effect against cerebral I/R injury. After 24h of MCAO surgery and behavioural assessment, the mice were sacrificed and damage to the brain area due to ischemia has been quantified using TTC staining method. As shown in Fig. 3, the sham treated mice showed no infarct area, while MCAO treated mice showed significant increase in infarct size as compared to sham. The infarct area was found to be significantly reduced in **8k** treated mice in dose-dependent manner as compared to MCAO treated mice.

<Figure 3>

The neural cell death in the cerebral injury induces inflammation in the injured brain areas and can exacerbate evolving tissue pathology. Therefore, in the next instance, we aimed to determine the effect of compound **8k** on the cytokines (TNF- α) and interleukins (IL- β and IL-6) and results are presented in Fig. 4. It has been found that, MCAO treated mice showed significant increase in concentration of examined cytokines and interleukins as compared to sham treated mice. Moreover, the level of TNF- α , IL- β and IL-6 were found to be reduced considerably in **8k** treated mice.

<Figure 4>

Oxidative stress followed by cerebral I/R injury is the main determinant of to induce neuro-inflammation due to the production of reactive oxygen species (ROS) (Mittal et al., 2014). Therefore, effect of compound **8k** was investigated on numerous oxidative stress markers, such as, SOD, GSH and MDA, Fig. 5. It has been found that, the level of GSH and activity SOD was reduced in MCAO treated mice together with increased MDA level. On the contrary, compound **8k** treated mice showed reduction of oxidative stress as evident by restoration of these biomarkers near to normal. This observation suggests that compound **8k** has significant antioxidant effect which might be responsible for protective action against neuro-inflammation and cerebral I/R injury.

<Figure 5>

Apoptosis mediated cell death due to DNA damage is considered as the main pathological feature of cerebral I/R injury. Various studies have shown that in response to oxidative stress, the B-cell lymphoma 2 (Bcl-2)-associated X protein (Bax) translocated from the cytoplasm to the mitochondria due to increased permeability of mitochondrial membrane. These Bcl-2 and Bax genes will govern the apoptotic process by acting as antiapoptotic and proapoptotic genes, respectively. Moreover, caspase-3 is the terminal protein of the cellular apoptosis cascade which can promote the cellular apoptosis (Liu et al., 2013). Thus it is valuable to investigate the effect of compound **8k** on the Bcl-2, Bax, and cleaved caspase-3 using western blot analysis. As observed in Fig. 6. The MCAO treated group showed increased expression of cleaved caspase-3 and Bax along with reduced Bcl-2 level. It was significant to note that, compound **8k** causes marked improvement in the expression of these tested apoptotic/pro-apoptotic protein near to normal.

<Figure 6>

Considering the significance of aberrant activation of NF- κ B in cerebral I/R injury, the last part of the study was aimed to investigate the effect of compound **8k** on the mediators of NF- κ B signalling cascade by western blot analysis (Schneider et al., 1999). As shown in Fig. 7, MCAO treated mice showed increased phosphorylation of I κ B α after reperfusion, whereas treatment with compound **8k** showed significant reduction of phosphorylation in dose-dependent manner. Moreover, compound **8k** also causes attenuation of phosphorylation and nuclear translocation of NF- κ Bp65, as compared to MCAO mice brains.

<Figure 7>

3. Material and methods

3.1. Chemistry

The chemicals used in the present study were obtained from Sigma Aldrich (USA). ^1H NMR spectra were recorded in *d*₆-DMSO on a Bruker Avance-400 NMR spectrometer with TMS as the internal reference. ^{13}C NMR spectra were recorded on a Bruker Avance-100 NMR spectrometer in DMSO on the same spectrometers with TMS as the internal reference. The multiplicity of a signal is indicated as: s – singlet, d – doublet, t – triplet, q – quartet, m – multiplet, br – broad, dd – doublet of doublets, *etc.* Coupling constants (*J*) are quoted in Hz and reported to the nearest 0.1 Hz. Infrared spectra were recorded as a neat thin film on a Perkin-Elmer Spectrum One FT-IR spectrometer using Universal ATR sampling accessories. Letters in the parentheses refer to the relative absorbency compared to the most intense peak: w – weak, less than 40%; m – medium, 40-75%; s – strong, greater than 75%. Melting points were obtained using an OptiMelt automated melting point system. MS spectra were recorded on an Agilent 1100 LC/MS.

Synthesis of compounds 3 (a-g), 4 (a-g) and 5 (a-g) were achieved by earlier reported procedure and the authenticity of compounds were assessed by FT-IR, mass and elemental analysis (Srivastava et al., 2015).

3.1.1. General procedure for the synthesis of title compounds 8 (a-g)

Corresponding substituted compound 5 (a-g) (0.1 mol), substituted benzaldehyde 6 (a-b) (0.1 mol) and mercaptoacetic acid 7 (0.1 mol) were refluxed in the presence of toluene for 8–12 h.

The product was filtered, washed with cold water and recrystallized with ethanol to afford the corresponding pure product 8 (a–g).

3.1.1.1. *2-(4-Chlorophenyl)-3-(4-morpholino-6-(phenylamino)-1,3,5-triazin-2-yl)thiazolidin-4-one (8a)*

Yield: 83 %; M.p: 218-219 °C; MW: 468.96 ; R_f : 0.64; FTIR (ν_{\max} ; cm^{-1} KBr): 3252 (N-H stretching), 3086 (C–H_{broad}), 2858 (CH₂ stretching), 1714 (C=O Stretching), 1684 (C=N_{aromatic}), 1648 (C=C), 1078 (C-N stretching), 817 (C-S stretching), 794 (C-Cl stretching), 624; ¹H NMR (400MHz, DMSO-d₆, TMS) δ ppm: 7.65 (d, 2H, J =1.49 Hz, Ar-H), 7.54 (d, 2H, J =1.57 Hz, Ar-H), 7.51 (d, 2H, J =1.47 Hz, Ar-H), 7.27 (d, 2H, J =1.44 Hz, Ar-H), 7.06 (t, 1H, J =1.23 Hz, Ar-H), 6.23 (s, 1H, Thiazolidine-H), 3.94 (s, 2H, Thiazolidine-H), 3.97 (s, 1H, NH-), 3.74-3.64 (m, 8H, CH₂×4, Morpholine-H); ¹³C NMR (100MHz, DMSO) δ ppm: 174.8, 171.3, 170.5, 169.2, 138.9, 137.4, 132.8, 130.1, 129.7, 128.7, 122.5, 117.9, 72.8, 66.3, 48.7, 33.5; Mass: 469.99 (M+H)⁺; Elemental analysis for C₂₂H₂₁ClN₆O₂S: Calculated: C, 56.35; H, 4.51; N, 17.92. Found: C, 56.38; H, 4.50; N, 17.94.

3.1.1.2. *2-(4-Chlorophenyl)-3-(4-((4-chlorophenyl)amino)-6-morpholino-1,3,5-triazin-2-yl)thiazolidin-4-one (8b)*

Yield: 71 %; M.p: 232-234 °C; MW: 503.40 ; R_f : 0.69; FTIR (ν_{\max} ; cm^{-1} KBr): 3258 (N-H stretching), 3081 (C–H_{broad}), 2856 (CH₂ stretching), 1712 (C=O Stretching), 1687 (C=N_{aromatic}), 1641 (C=C), 1072 (C-N stretching), 812 (C-S stretching), 791 (C-Cl stretching), 627; ¹H NMR (400MHz, DMSO-d₆, TMS) δ ppm: 7.75 (d, 2H, J =1.54 Hz, Ar-H), 7.65 (d, 2H, J =1.49 Hz, Ar-H), 7.54 (d, 2H, J =1.55 Hz, Ar-H), 7.42 (d, 2H, J =1.64 Hz, Ar-H), 6.25 (s, 1H, Thiazolidine-H), 3.95 (s, 2H, Thiazolidine-H), 3.99 (s, 1H, NH-), 3.76-3.65 (m, 8H, CH₂×4, Morpholine-H); ¹³C NMR (100MHz, DMSO) δ ppm: 182.9, 171.3, 167.5, 164.4, 137.6, 137.1, 132.8, 130.2, 129.8, 128.8, 127.7, 122.1, 72.8, 66.4, 48.7, 33.6; Mass: 504.43 (M+H)⁺; Elemental analysis for C₂₂H₂₀Cl₂N₆O₂S: Calculated: C, 52.49; H, 4.00; N, 16.69. Found: C, 52.51; H, 4.04; N, 16.72.

3.1.1.3. *2-(4-Chlorophenyl)-3-(4-((4-fluorophenyl)amino)-6-morpholino-1,3,5-triazin-2-yl)thiazolidin-4-one (8c)*

Yield: 78 %; M.p: 225-226 °C; MW: 486.95 ; R_f : 0.79; FTIR (ν_{\max} ; cm^{-1} KBr): 3254 (N-H stretching), 3087 (C–H_{broad}), 2852 (CH₂ stretching), 1709 (C=O Stretching), 1689 (C=N_{aromatic}),

1645 (C=C), 1156 (C-F stretching), 1076 (C-N stretching), 816 (C-S stretching), 793 (C-Cl stretching), 637; ¹H NMR (400MHz, DMSO-d₆, TMS) δ ppm: 7.72 (d, 2H, *J*=1.84 Hz, Ar-H), 7.66 (d, 2H, *J*=1.46 Hz, Ar-H), 7.56 (d, 2H, *J*=1.53 Hz, Ar-H), 7.06 (d, 2H, *J*=1.59 Hz, Ar-H), 6.24 (s, 1H, Thiazolidine-H), 3.96 (s, 2H, Thiazolidine-H), 3.98 (s, 1H, NH-), 3.75-3.63 (m, 8H, CH₂×4, Morpholine-H); ¹³C NMR (100MHz, DMSO) δ ppm: 182.8, 171.3, 167.4, 164.3, 157.4, 137.5, 134.5, 132.8, 130.2, 128.9, 120.7, 116.4, 72.7, 66.4, 48.8, 33.7; Mass: 487.93 (M+H)⁺; Elemental analysis for C₂₂H₂₀ClFN₆O₂S: Calculated: C, 54.26; H, 4.14; N, 17.26. Found: C, 54.27; H, 4.12; N, 17.29.

3.1.1.4. 2-(4-Chlorophenyl)-3-(4-morpholino-6-((4-nitrophenyl)amino)-1,3,5-triazin-2-yl)thiazolidin-4-one (8d)

Yield: 84 %; M.p: 245-247 °C; MW: 513.96 ; R_f: 0.74; FTIR (ν_{max}; cm⁻¹ KBr): 3258 (N-H stretching), 3083 (C-H_{broad}), 2856 (CH₂ stretching), 1708 (C=O Stretching), 1685 (C=N_{aromatic}), 1648 (C=C), 1538 (NO₂ stretching), 1078 (C-N stretching), 817 (C-S stretching), 792 (C-Cl stretching), 635; ¹H NMR (400MHz, DMSO-d₆, TMS) δ ppm: 8.12 (d, 2H, *J*=1.82 Hz, Ar-H), 7.64 (d, 2H, *J*=1.48 Hz, Ar-H), 7.55 (d, 2H, *J*=1.56 Hz, Ar-H), 7.34 (d, 2H, *J*=2.24 Hz, Ar-H), 6.25 (s, 1H, Thiazolidine-H), 3.95 (s, 2H, Thiazolidine-H), 3.97 (s, 1H, NH-), 3.74-3.66 (m, 8H, CH₂×4, Morpholine-H); ¹³C NMR (100MHz, DMSO) δ ppm: 174.7, 171.3, 170.8, 169.4, 145.1, 137.9, 137.4, 132.7, 130.2, 128.7, 124.7, 119.2, 72.8, 66.5, 48.7, 33.6 ; Mass: 514.98 (M+H)⁺; Elemental analysis for C₂₂H₂₀ClN₇O₄S: Calculated: C, 51.41; H, 3.92; N, 19.08. Found: C, 51.40; H, 3.95; N, 19.06.

3.1.1.5. 2-(4-Fluorophenyl)-3-(4-((4-hydroxyphenyl)amino)-6-morpholino-1,3,5-triazin-2-yl)thiazolidin-4-one (8e)

Yield: 79 %; M.p: 238-239 °C; MW: 484.96 ; R_f: 0.70; FTIR (ν_{max}; cm⁻¹ KBr): 3262 (N-H stretching), 3225 (O-H stretching), 3087 (C-H_{broad}), 2859 (CH₂ stretching), 1719 (C=O Stretching), 1685 (C=N_{aromatic}), 1647 (C=C), 1342 (O-H bending), 1079 (C-N stretching), 813 (C-S stretching), 792 (C-Cl stretching), 631; ¹H NMR (400MHz, DMSO-d₆, TMS) δ ppm: 7.67 (d, 2H, *J*=1.49 Hz, Ar-H), 7.54 (d, 2H, *J*=1.57 Hz, Ar-H), 7.27 (d, 2H, *J*=1.38 Hz, Ar-H), 6.67 (d, 2H, *J*=2.63 Hz, Ar-H), 6.24 (s, 1H, Thiazolidine-H), 5.46 (s, 1H, Ar-OH), 3.97 (s, 2H, Thiazolidine-H), 3.98 (s, 1H, NH-), 3.75-3.63 (m, 8H, CH₂×4, Morpholine-H); ¹³C NMR (100MHz, DMSO) δ ppm: 182.9, 171.3, 167.5, 164.5, 148.6, 137.4, 132.8, 131.5, 130.1, 128.7, 122.1, 116.7, 72.8, 66.4,

48.8, 33.6 ; Mass: 485.95 (M+H)⁺; Elemental analysis for C₂₂H₂₁ClN₆O₃S: Calculated: C, 54.49; H, 4.36; N, 17.33. Found: C, 54.52; H, 4.34; N, 17.31.

3.1.1.6. *2-(4-Fluorophenyl)-3-(4-((4-methoxyphenyl)amino)-6-morpholino-1,3,5-triazin-2-yl)thiazolidin-4-one (8f)*

Yield: 67 %; M.p: 249-251 °C; MW: 498.99 ; R_f: 0.65; FTIR (ν_{max}; cm⁻¹ KBr): 3268 (N-H stretching), 3084 (C-H broad), 2851 (CH₂ stretching), 2824 (OCH₃ stretching), 1715 (C=O Stretching), 1681 (C=N aromatic), 1649 (C=C), 1074 (C-N stretching), 812 (C-S stretching), 793 (C-Cl stretching), 638; ¹H NMR (400MHz, DMSO-d₆, TMS) δ ppm: 7.65 (d, 2H, J=1.47 Hz, Ar-H), 7.56 (d, 2H, J=1.59 Hz, Ar-H), 7.32 (d, 2H, J=1.68 Hz, Ar-H), 6.62 (d, 2H, J=2.72 Hz, Ar-H), 6.23 (s, 1H, Thiazolidine-H), 3.96 (s, 2H, Thiazolidine-H), 3.99 (s, 1H, NH-), 3.74-3.62 (m, 8H, CH₂×4, Morpholine-H), 3.71 (s, 3H, OCH₃); ¹³C NMR (100MHz, DMSO) δ ppm: 182.9, 171.3, 167.5, 164.2, 153.4, 137.5, 132.8, 131.2, 130.2, 128.9, 121.8, 115.2, 72.8, 66.5, 55.9, 48.9, 33.5; Mass: 499.97 (M+H)⁺; Elemental analysis for C₂₃H₂₃ClN₆O₃S: Calculated: C, 55.36; H, 4.65; N, 16.84. Found: C, 55.34; H, 4.69; N, 16.85.

3.1.1.7. *2-(4-Fluorophenyl)-3-(4-morpholino-6-(p-tolylamino)-1,3,5-triazin-2-yl)thiazolidin-4-one (8g)*

Yield: 76 %; M.p: 241-242 °C; MW: 482.99 ; R_f: 0.78; FTIR (ν_{max}; cm⁻¹ KBr): 3262 (N-H stretching), 3087 (C-H broad), 2952 (alkyl C-H stretching), 2852 (CH₂ stretching), 1718 (C=O Stretching), 1685 (C=N aromatic), 1642 (C=C), 1467 (CH₃ bending), 1078 (C-N stretching), 814 (C-S stretching), 792 (C-Cl stretching), 632; ¹H NMR (400MHz, DMSO-d₆, TMS) δ ppm: 7.67 (d, 2H, J=1.48 Hz, Ar-H), 7.55 (d, 2H, J=1.56 Hz, Ar-H), 7.34 (d, 2H, J=1.34 Hz, Ar-H), 7.07 (d, 2H, J=1.59 Hz, Ar-H), 6.24 (s, 1H, Thiazolidine-H), 3.96 (s, 2H, Thiazolidine-H), 3.98 (s, 1H, NH-), 3.76-3.64 (m, 8H, CH₂×4, Morpholine-H), 2.24 (s, 3H, CH₃); ¹³C NMR (100MHz, DMSO) δ ppm: 174.7, 171.3, 170.8, 169.4, 137.5, 135.9, 132.6, 131.2, 130.2, 129.8, 128.8, 120.3, 72.8, 66.4, 48.7, 33.6, 21.4; Mass: 483.94 (M+H)⁺; Elemental analysis for C₂₃H₂₃ClN₆O₂S: Calculated: C, 57.20; H, 4.80; N, 17.40. Found: C, 57.23; H, 4.78; N, 17.45.

3.1.1.8. *2-(4-Fluorophenyl)-3-(4-morpholino-6-(phenylamino)-1,3,5-triazin-2-yl)thiazolidin-4-one (8h)*

Yield: 68 %; M.p: 196-197 °C; MW: 452.51 ; R_f : 0.69; FTIR (ν_{\max} ; cm^{-1} KBr): 3259 (N-H stretching), 3089 (C-H_{broad}), 2851 (CH₂ stretching), 1709 (C=O Stretching), 1687 (C=N_{aromatic}), 1646 (C=C), 1154 (C-F stretching), 1072 (C-N stretching), 814 (C-S stretching), 629; ¹H NMR (400MHz, DMSO-d₆, TMS) δ ppm: 7.51 (d, 2H, J =1.47 Hz, Ar-H), 7.46 (d, 2H, J =1.33 Hz, Ar-H), 7.27 (d, 2H, J =1.42 Hz, Ar-H), 7.09 (d, 2H, J =1.25 Hz, Ar-H), 7.05 (t, 1H, J =1.24 Hz, Ar-H), 6.20 (s, 1H, Thiazolidine-H), 3.95 (s, 2H, Thiazolidine-H), 3.98 (s, 1H, NH-), 3.75-3.63 (m, 8H, CH₂×4, Morpholine-H); ¹³C NMR (100MHz, DMSO) δ ppm: 174.8, 171.3, 170.8, 169.5, 161.4, 138.9, 134.9, 130.4, 129.6, 122.6, 117.8, 115.4, 72.9, 66.4, 48.9, 33.7; Mass: 469.99 (M+H)⁺; Elemental analysis for C₂₂H₂₁FN₆O₂S: Calculated: C, 58.39; H, 4.68; N, 18.57. Found: C, 58.43; H, 4.67; N, 18.58.

3.1.1.9. *3-(4-((4-Chlorophenyl)amino)-6-morpholino-1,3,5-triazin-2-yl)-2-(4-fluorophenyl)thiazolidin-4-one (8i)*

Yield: 73 %; M.p: 211-212 °C; MW: 486.95 ; R_f : 0.74; FTIR (ν_{\max} ; cm^{-1} KBr): 3262 (N-H stretching), 3088 (C-H_{broad}), 2857 (CH₂ stretching), 1715 (C=O Stretching), 1689 (C=N_{aromatic}), 1645 (C=C), 1156 (C-F stretching), 1078 (C-N stretching), 811 (C-S stretching), 798 (C-Cl stretching), 621; ¹H NMR (400MHz, DMSO-d₆, TMS) δ ppm: 7.78 (d, 2H, J =1.51 Hz, Ar-H), 7.41 (d, 2H, J =1.64 Hz, Ar-H), 7.46 (d, 2H, J =1.34 Hz, Ar-H), 7.09 (d, 2H, J =1.25 Hz, Ar-H), 6.21 (s, 1H, Thiazolidine-H), 3.94 (s, 2H, Thiazolidine-H), 3.97 (s, 1H, NH-), 3.73-3.61 (m, 8H, CH₂×4, Morpholine-H); ¹³C NMR (100MHz, DMSO) δ ppm: 182.7, 171.4, 167.5, 164.5, 161.4, 137.2, 134.9, 130.4, 129.6, 127.8, 122.1, 115.5, 72.8, 66.4, 48.9, 33.6; Mass: 504.43 (M+H)⁺; Elemental analysis for C₂₂H₂₀ClFN₆O₂S: Calculated: C, 54.26; H, 4.14; N, 17.26. Found: C, 54.29; H, 4.09; N, 17.28.

3.1.1.10. *2-(4-Fluorophenyl)-3-(4-((4-fluorophenyl)amino)-6-morpholino-1,3,5-triazin-2-yl)thiazolidin-4-one (8j)*

Yield: 84 %; M.p: 189-190 °C; MW: 470.50 ; R_f : 0.87; FTIR (ν_{\max} ; cm^{-1} KBr): 3259 (N-H stretching), 3083 (C-H_{broad}), 2851 (CH₂ stretching), 1706 (C=O Stretching), 1687 (C=N_{aromatic}), 1648 (C=C), 1159 (C-F stretching), 1073 (C-N stretching), 819 (C-S stretching), 645; ¹H NMR (400MHz, DMSO-d₆, TMS) δ ppm: 7.74 (d, 2H, J =1.81 Hz, Ar-H), 7.46 (d, 2H, J =1.32 Hz, Ar-H), 7.09 (d, 2H, J =1.24 Hz, Ar-H), 7.01 (d, 2H, J =1.56 Hz, Ar-H), 6.23 (s, 1H, Thiazolidine-H), 3.92 (s, 2H, Thiazolidine-H), 3.99 (s, 1H, NH-), 3.72-3.65 (m, 8H, CH₂×4, Morpholine-H); ¹³C

NMR (100MHz, DMSO) δ ppm:182.6, 171.4, 167.7, 164.4, 161.2, 157.5, 134.8, 134.5, 130.5, 120.7, 116.4, 115.6, 72.8, 66.4, 48.9, 33.5; Mass: 471.56 (M+H)⁺; Elemental analysis for C₂₂H₂₀F₂N₆O₂S: Calculated: C, 56.16; H, 4.28; N, 17.86. Found: C, 56.15; H, 4.24; N, 17.87.

3.1.1.11. *2-(4-Fluorophenyl)-3-(4-morpholino-6-((4-nitrophenyl)amino)-1,3,5-triazin-2-yl)thiazolidin-4-one (8k)*

Yield: 81 %; M.p: 252-253 °C; MW: 497.51 ; R_f: 0.77; FTIR (ν_{\max} ; cm⁻¹ KBr): 3254 (N-H stretching), 3087 (C-H_{broad}), 2858 (CH₂ stretching), 1713 (C=O Stretching), 1686 (C=N_{aromatic}), 1642 (C=C), 1534 (NO₂ stretching), 1156 (C-F stretching), 1075 (C-N stretching), 819 (C-S stretching), 648; ¹H NMR (400MHz, DMSO-d₆, TMS) δ ppm: 8.14 (d, 2H, *J*=1.84 Hz, Ar-H), 7.47 (d, 2H, *J*=1.35 Hz, Ar-H), 7.34 (d, 2H, *J*=2.24 Hz, Ar-H), 7.09 (d, 2H, *J*=2.21 Hz, Ar-H), 6.22 (s, 1H, Thiazolidine-H), 3.93 (s, 2H, Thiazolidine-H), 3.98 (s, 1H, NH-), 3.75-3.62 (m, 8H, CH₂×4, Morpholine-H); ¹³C NMR (100MHz, DMSO) δ ppm:176.7, 171.4, 170.8, 169.2, 161.4, 145.1, 137.9, 134.9, 130.4, 124.8, 119.2, 115.5, 72.8, 66.4, 48.8, 33.6; Mass: 498.12 (M+H)⁺; Elemental analysis for C₂₂H₂₀FN₇O₄S: Calculated: C, 53.11; H, 4.05; N, 19.71. Found: C, 53.09; H, 4.08; N, 19.75.

3.1.1.12. *2-(4-Fluorophenyl)-3-(4-((4-hydroxyphenyl)amino)-6-morpholino-1,3,5-triazin-2-yl)thiazolidin-4-one (8l)*

Yield: 86 %; M.p: 201-203 °C; MW: 468.51 ; R_f: 0.76; FTIR (ν_{\max} ; cm⁻¹ KBr): 3268 (N-H stretching), 3223 (O-H stretching), 3081 (C-H_{broad}), 2857 (CH₂ stretching), 1713 (C=O Stretching), 1686 (C=N_{aromatic}), 1649 (C=C), 1348 (O-H bending), 1159 (C-F stretching), 1072 (C-N stretching), 814 (C-S stretching), 648; ¹H NMR (400MHz, DMSO-d₆, TMS) δ ppm: 7.48 (d, 2H, *J*=1.34 Hz, Ar-H), 7.27 (d, 2H, *J*=1.38 Hz, Ar-H), 7.08 (d, 2H, *J*=1.26 Hz, Ar-H), 6.68 (d, 2H, *J*=2.65 Hz, Ar-H), 6.20 (s, 1H, Thiazolidine-H), 5.52 (s, 1H, Ar-OH), 3.92 (s, 2H, Thiazolidine-H), 3.96 (s, 1H, NH-), 3.72-3.68 (m, 8H, CH₂×4, Morpholine-H); ¹³C NMR (100MHz, DMSO) δ ppm:182.7, 171.3, 167.6, 164.4, 161.2, 148.5, 134.9, 131.6, 130.3, 122.1, 116.8, 115.5, 72.8, 66.4, 48.9, 33.5; Mass: 469.52 (M+H)⁺; Elemental analysis for C₂₂H₂₁FN₆O₃S: Calculated: C, 56.40; H, 4.52; N, 17.94. Found: C, 56.42; H, 4.56; N, 17.93.

3.1.1.13. *2-(4-Fluorophenyl)-3-(4-((4-methoxyphenyl)amino)-6-morpholino-1,3,5-triazin-2-yl)thiazolidin-4-one (8m)*

Yield: 85 %; M.p: 228-229 °C; MW: 482.53 ; R_f : 0.79; FTIR (ν_{\max} ; cm^{-1} KBr): 3263 (N-H stretching), 3085 (C-H broad), 2852 (CH₂ stretching), 2826 (OCH₃ stretching), 1717 (C=O Stretching), 1683 (C=N aromatic), 1645 (C=C), 1154 (C-F stretching), 1076 (C-N stretching), 815 (C-S stretching), 635; ¹H NMR (400MHz, DMSO-d₆, TMS) δ ppm: 7.48 (d, 2H, J =1.35 Hz, Ar-H), 7.32 (d, 2H, J =1.67 Hz, Ar-H), 7.09 (d, 2H, J =1.25 Hz, Ar-H), 6.64 (d, 2H, J =2.75 Hz, Ar-H), 6.21 (s, 1H, Thiazolidine-H), 3.94 (s, 2H, Thiazolidine-H), 3.96 (s, 1H, NH-), 3.77-3.63 (m, 8H, CH₂×4, Morpholine-H), 3.76 (s, 3H, OCH₃); ¹³C NMR (100MHz, DMSO) δ ppm: 182.5, 171.4, 167.5, 164.1, 161.2, 153.4, 134.9, 131.3, 130.2, 121.8, 115.6, 115.1, 72.8, 66.4, 55.8, 48.8, 33.5; Mass: 483.57 (M+H)⁺; Elemental analysis for C₂₃H₂₃FN₆O₃S: Calculated: C, 57.25; H, 4.80; N, 17.42. Found: C, 57.27; H, 4.81; N, 17.40.

3.1.1.14. 2-(4-Fluorophenyl)-3-(4-morpholino-6-(p-tolylamino)-1,3,5-triazin-2-yl)thiazolidin-4-one (8n)

Yield: 72 %; M.p: 213-214 °C; MW: 466.54 ; R_f : 0.71; FTIR (ν_{\max} ; cm^{-1} KBr): 3269 (N-H stretching), 3083 (C-H broad), 2954 (alkyl C-H stretching), 2856 (CH₂ stretching), 1714 (C=O Stretching), 1682 (C=N aromatic), 1647 (C=C), 1469 (CH₃ bending), 1157 (C-F stretching), 1072 (C-N stretching), 814 (C-S stretching), 639; ¹H NMR (400MHz, DMSO-d₆, TMS) δ ppm: 7.49 (d, 2H, J =1.32 Hz, Ar-H), 7.34 (d, 2H, J =1.29 Hz, Ar-H), 7.09 (d, 2H, J =1.25 Hz, Ar-H), 7.05 (d, 2H, J =1.54 Hz, Ar-H), 6.23 (s, 1H, Thiazolidine-H), 3.92 (s, 2H, Thiazolidine-H), 3.97 (s, 1H, NH-), 3.74-3.62 (m, 8H, CH₂×4, Morpholine-H), 2.21 (s, 3H, CH₃); ¹³C NMR (100MHz, DMSO) δ ppm: 174.8, 171.2, 170.8, 169.4, 161.2, 135.8, 134.8, 131.3, 130.1, 129.8, 120.4, 115.5, 72.8, 66.4, 48.9, 33.6, 21.3; Mass: 467.56 (M+H)⁺; Elemental analysis for C₂₃H₂₃FN₆O₂S: Calculated: C, 59.21; H, 4.97; N, 18.01. Found: C, 59.25; H, 4.96; N, 18.02.

3.2. *In vitro* NF- κ B transcription inhibitory activity

RAW264.7 macrophages were purchased from American Type Culture Collection (ATCC, USA). Cells were cultured in DMEM with 10% FBS, 100 mg mL⁻¹ streptomycin and 100 U mL⁻¹ penicillin in humidified 5% CO₂ at 37 °C. The 80% confluency of RAW264.7 cells was achieved in six well plates and transfected with 1 mg of the NF- κ B reporter construct, along with 0.5 mg of pSVGal plasmid using Lipofect-AMINE 2000 (Invitrogen) in Opti-MEM medium (Gibco). After 24 hours of transfection, cells were treated with LPS or target derivatives (100 μ M) for an additional 2 h, and then lysed using the reporter lysis buffer (Promega). Luciferase assays were

performed using 20 μ L of cell extract and 100 μ L of luciferin substrate (Promega), and the luciferase activity was measured using a Dual-Luciferase Reporter Assay System (Promega) according to the manufacturer's instructions. Luciferase and *Renilla* activities were measured by an Orion microplate luminometer (Berthold detection systems).

3.3. Pharmacological Activity

3.3.1. Animals

The C57/BL6 male mice were obtained from the Institutional animal house and housed in controlled environment with *ad libitum* supply of food and water. The animals were kept under in alternate light and dark cycles of 12 h. The study was approved reviewed and approved by the Animal Ethical and Welfare Committee of People's Hospital of Nanjing Medical University, China.

3.3.2. Animal model of cerebral ischemia

No food and water for 12 h before the MCAO surgery was given to animals. The MCAO surgery was performed as per the earlier reported procedure. Towards this, the mice were anesthetized with an intraperitoneal injection of 10% chloral hydrate (350 mg/kg) and fixed on the surgery board in the supine position. The left carotid region was exposed through a midline cervical incision; the external carotid artery and the common carotid artery were exposed. A non-traumatic microvascular clamp was introduced from the carotid bifurcation into the internal carotid artery, thereby occluding the origin of the middle cerebral artery. After a 2-hours occlusion, reperfusion was initiated by withdrawal of the clamp. Finally, the incision was sutured and the animal was allowed to recover from anesthesia. During the operation, the rectal temperature of mice was maintained at 37 $^{\circ}$ C using a heating lamp. Sham operated group received the same procedure but without MCA occlusion. The animals were allowed to recover from anesthesia prior to being returned to their original housing.

3.3.3. Drug treatment

The lethal dose of compound **8k** was found to be more than 2000mg/kg in mice as per the sub acute toxicity assay according to OECD guidelines. Therefore, compound 8k was used in the dose of 5, 10 and 15 mg/kg in mice. The compounds were suspended in 2% carboxy methyl cellulose (CMC) for administration. The compounds were administered intraperitoneally immediately and

after 12 h of MCAO surgery. The sham and MCAO treated mice administered with normal saline. The animals were sacrificed after reperfusion for 24 h and brain infarct volume was determined using TTC staining. On the other hand, ischemic area of brain containing the cortex and hippocampus were separated and then lysed for the determination of inflammatory cytokine and western blot analysis.

3.3.4. Assessment of neurological deficit

The effect of compound 8k was determined on the neurological dysfunction of mice after 24h of MCAO surgery by an observer blinded to the treatment of experimental animals using a 5-point neurological score. The score was assigned as follows, 0 for no deficit; 1 for flexion of contralateral forelimb; 2 for decrease in resistance toward the contralateral plane; 3 for circling monolaterally; and 4 for labored or absent ambulation. Higher scores represented more serious dysfunction.

3.3.5. Evaluation of cerebral edema

For measurement of cerebral edema, the brains were rapidly excised onto ice after ischemia reperfusion. Immediately, weigh the brain sample to get the wet weight (ww) and then the brain tissue sample was dried at 60 °C for 48 h to get the dry weight (dw). After that, the brain water content was calculated as follows: The cerebral edema= $[(ww-dw)/(ww)] \times 100\%$.

3.3.6. Histological examination

The H and E staining of brain coronal sections were performed after were fixed in 10% neutral buffered formalin for 48 h then the samples were processed to get 4 μm paraffin embedded sections. Then, the sections were stained with hematoxylin and eosin (H&E). The infarct areas were determined, photographed and calculated in each histopathological section by using Lieca Qwin 500 Image Analyzer (Leica, Cambridge, England).

3.3.7. Evaluation of mice brain infarct area

Briefly, the mice brains were excised, freezed and cutted into coronal sections of 2-mm. The 2% solution of TTC in saline phosphate was used to incubate the brain slices at 37 °C for 30 min. The different colouring pattern of brain was recorded with the help of digital camera into two distinct color zones, such as red and un-stained region which denotes normal tissue and infarct

region, respectively. The volume of the whole brain and the infarct tissue was determined with Image-Pro Plus software USA.

3.3.8. *Detection of inflammatory cytokines in brain tissue*

The effect of compound 8k on the TNF- α , IL- β and IL-6 using the ELISA kits as per the manufacturer instruction (R&D Systems ELISA kit Minneapolis MN 55413, USA).

3.4. *Western blot analysis*

Protein levels were determined using a BCA protein assay kit (Thermo Fisher Scientific). Protein extract (50 μ g) was resolved by 12% SDS-PAGE electrophoresis and electrotransferred onto a nitrocellulose membrane. The membrane was blocked using TrisPBS (TPBS) with Tween 20 and 5% skimmed milk and probed with primary antibodies: Next, an anti-rabbit secondary antibody conjugated to horseradish peroxidase (1: 10 000; Abcam/Cell Signaling Technology) in TPBS was added and incubated at 37°C for 1 h. Bands were visualized using an enhanced chemiluminescence image analyzer, and protein levels were quantified using Image-Pro Plus software (Media Cybernetics, Inc., MD, USA).

3.5. *Statistical analysis*

All data are presented as mean \pm SD of three independent experiments. Data were statistically analyzed by one-way analysis followed by the by a Tukey's *post hoc* test using statistical software GraphPad Prism 5.0 (California, USA). The P value < 0.05 was considered as statistically significant.

4. **Conclusion**

As a concluding remark, the present study showed the development of thiazolidin-4-one-1,3,5-triazine derivatives as protective agent against cerebral ischemia/reperfusion injury. The molecules showed excellent *in-vitro* inhibition of NF- κ B activation in RAW264.7 cells. The most potent NF- κ B inhibitor (**8k**) showed neuro-protective effect in mice mediated through attenuation of inflammation, oxidative stress and apoptosis. Compound **8k** also showed inhibition of activation of NF- κ B pathway in western blot analysis. In the SAR analysis, electron-withdrawing group found more active than their electron donating counterparts which have encouraged us to

investigate additional novel lead scaffolds exhibiting potent neuro-protective activity through inactivation of NF- κ B.

Competing interests

The authors declare that they have no competing interests.

Data availability statement

The data that support the findings of this study are available from the corresponding author upon reasonable request.

References

- Astrup, J., Siesjö, B. K., Symon, L. (1981). Thresholds in cerebral ischemia — the ischemic penumbra. *Stroke.*, *12*, 723–725.
- Avery, M. B., Ogilvy, C. S., Mitha, A. P. (2016). Cerebrovascular Disease. In *The Curated Reference Collection in Neuroscience and Biobehavioral Psychology*. 801–806. doi:10.1016/B978-0-12-809324-5.02031-9.
- Broughton, B.R., Reutens, D.C., Sobey, C.G. (2009). Apoptotic mechanisms after cerebral ischemia. *Stroke*, *40*(5), e331-339. doi: 10.1161/STROKEAHA.108.531632.
- Chan, P. H. (2001). Reactive oxygen radicals in signaling and damage in the ischemic brain. *J. Cereb. Blood Flow Metab.*, *21*, 2–14. DOI: 10.1097/00004647-200101000-00002
- Chiang, T., Messing, R.O., Chou, W.H. (2011). Mouse model of middle cerebral artery occlusion. *J Vis Exp*. 13(48) doi: 10.3791/2761.
- Conner, E.M., Grisham, M.B. (1996). Inflammation, free radicals and antioxidants. *Nutrition*, *12*, 274–277. DOI: 10.1016/s0899-9007(96)00000-8
- Dao, P., Smith, N., Tomkiewicz-Raulet, C., Yen-Pon, E., Camacho-Artacho, M., Lietha, D.,

Herbeuval, J.P., Coumoul, X., Garbay, C., Chen, H. (2015). Design, synthesis, and evaluation of novel imidazo[1,2-a][1,3,5]triazines and their derivatives as focal adhesion kinase inhibitors with antitumor activity. *J. Med. Chem.* *58*, 237-2 51. doi: 10.1021/jm500784e.

Dwivedi, J., Devi, K., Asmat, Y., Jain, S., Sharma, S. (2016). Synthesis, characterization, antibacterial and antiepileptic studies of some novel thiazolidinone derivatives. *J. Saudi Chem. Soc.* *20*, S16-S20. <https://doi.org/10.1016/j.jscs.2012.09.001>

Halliwell, B. (2006). Oxidative stress and neurodegeneration: Where are we now? *J. Neurochem.* *97*, 1634–1658. DOI: 10.1111/j.1471-4159.2006.03907.x

Hayden, M. S., Ghosh, S. (2004). Signaling to NF- κ B. *Genes Dev.* *18*, 2195–2224. doi: 10.1101/gad.1228704

Hodous, B.L., Geuns-Meyer, S.D., Hughes, P.E., Albrecht, B.K., Bellon, S., Bready, J., Caenepeel, S., Cee, V.J., Chaffee, S.C., Coxon, A., Emery, M., Fretland, J., Gallant, P., Gu, Y., Hoffman, D., Johnson, R.E., Kendall, R., Kim, J.L., Long, A.M., Morrison, M., Olivieri, P.R., Patel, V.F., Polverino, A., Rose, P., Tempest, P., Wang, L., Whittington, D.A., Zhao, H. (2007). Evolution of a highly selective and potent 2-(pyridin-2-yl)-1,3,5-triazine Tie-2 kinase inhibitor. *J. Med. Chem.* *50*, 611-626. DOI: 10.1021/jm061107l.

Huang, J., Upadhyay, U.M., Tamargo, R.J. (2006). Inflammation in stroke and focal cerebral ischemia. *Surg Neurol.* *66*(3), 232-245. doi: 10.1016/j.surneu.2005.12.028

Jin, R., Yang, G., Li, G. (2010). Inflammatory mechanisms in ischemic stroke: role of inflammatory cells. *J Leukoc Biol.* *87*(5), 779-89. doi: 10.1189/jlb.1109766.

Joseph, A., Shah, C.S., Kumar, S.S., Alex, A.T., Maliyakkal, N., Moorkoth, S., Mathew, J.E. (2013). Synthesis, in vitro anticancer and antioxidant activity of thiadiazole substituted thiazolidin-4-ones. *Acta Pharm.*, *63*, 397-408. doi: 10.2478/acph-2013-0028.

Karin, M., Ben-Neriah, Y. (2000). Phosphorylation meets ubiquitination: the control of NF-

[kappa]B activity. *Annu Rev Immunol.* 18, 621-663. doi:
10.1146/annurev.immunol.18.1.621

Lakhan, S.E., Kirchgessner, A., Hofer, M. (2009). Inflammatory mechanisms in ischemic stroke: Therapeutic approaches. *J. Transl. Med.* 7, 97. doi: 10.1186/1479-5876-7-97.

Liu, F., McCullough, L. D. (2011). Middle cerebral artery occlusion model in rodents: methods and potential pitfalls. *Journal of biomedicine & biotechnology*, 2011, 464701.
<https://doi.org/10.1155/2011/464701>

Liu, G., Wang, T., Wang, T., Song, J., Zhou, Z. (2013). Effects of apoptosis-related proteins caspase-3, Bax and Bcl-2 on cerebral ischemia rats. *Biomed. Reports.*, 1, 861-867. DOI: 10.3892/br.2013.153

Liu, T., Zhang, L., Joo, D., Sun, S.C. (2017). NF- κ B signaling in inflammation. *Signal Transduct. Target. Ther.* 2, pii: 17023. doi: 10.1038/sigtrans.2017.23.

Lordan, R., Tsoupras, A., Zabetakis I. (2019). In *The Impact of Nutrition and Statins on Cardiovascular Diseases*, 23–51. <https://doi.org/10.1016/B978-0-12-813792-5.00002-1>

Mittal, M., Siddiqui, M.R., Tran, K., Reddy, S.P., Malik, A.B. (2014). Reactive oxygen species in inflammation and tissue injury. *Antioxidants Redox Signal.* 20, 1126–1167. doi: 10.1089/ars.2012.5149.

Mogilski, S., Kubacka, M., Łażewska, D., Więcek, M., Głuch-Lutwin, M., Tyszka-Czochara, M., Bukowska-Strakova, K., Filipek, B., Kieć-Kononowicz, K. (2017). Aryl-1,3,5-triazine ligands of histamine H4 receptor attenuate inflammatory and nociceptive response to carrageen, zymosan and lipopolysaccharide. *Inflamm. Res.* 66, 79- 95. doi: 10.1007/s00011-016-0997-z.

Murugesan, V., Makwana, N., Suryawanshi, R., Saxena, R., Tripathi, R., Paranjape, R., Kulkarni, S., Katti, S.B. (2014). Rational design and synthesis of novel thiazolidin-4-ones as non-nucleoside HIV-1 reverse transcriptase inhibitors. *Bioorganic Med. Chem.* 22, 3159-3170.

doi: 10.1016/j.bmc.2014.04.018.

Popowycz, F., Fournet, G., Schneider, C., Bettayeb, K., Ferandin, Y., Lamigeon, C., Tirado, O.M., Mateo-Lozano, S., Notario, V., Colas, P., Bernard, P., Meijer, L., Joseph, B. (2009). Pyrazolo[1,5-a]-1,3,5-triazine as a purine bioisostere: access to potent cyclin-dependent kinase inhibitor (R)-roscovitine analogue. *J. Med. Chem.*, 52, 655-63. doi: 10.1021/jm801340z.

Rashid, M., Husain, A., Shaharyar, M., Mishra, R., Hussain, A., Afzal, O. (2014). Design and synthesis of pyrimidine molecules endowed with thiazolidin-4-one as new anticancer agents. *Eur. J. Med. Chem.*, 83, 630-645. doi: 10.1016/j.ejmech.2014.06.033.

Ridder, D. A., Schwaninger, M. (2009). NF- κ B signaling in cerebral ischemia. *Neuroscience*, 158, 995–1006. doi: 10.1016/j.neuroscience.2008.07.007.

Schneider, A., Martin-Villalba, A., Weih, F., Vogel, J., Wirth, T., Schwaninger, M. (1999). NF- κ B is activated and promotes cell death in focal cerebral ischemia. *Nat. Med.*, 5, 554-559. DOI: 10.1038/8432

Shih RH, Wang CY, Yang CM. (2015). NF- κ B signaling pathways in neurological inflammation: A mini review. *Front. Mol. Neurosci.* 8, 77. doi: 10.3389/fnmol.2015.00077.

Singh, U.P., Bhat, H.R., Gahtori, P. (2012). Antifungal activity, SAR and physicochemical correlation of some thiazole-1,3,5-triazine derivatives. *J. Mycol. Med.* 22, 134-141. doi: 10.1016/j.mycmed.2011.12.073.

Singh, U.P., Bhat, H.R., Gahtori, P., Singh, R.K. (2013). Hybrid phenylthiazole and 1,3,5-triazine target cytosolic leucyl-tRNA synthetase for antifungal action as revealed by molecular docking studies. *Silico Pharmacol.* 1, 3. doi: 10.1186/2193-9616-1-3.

Singh, B., Bhat, H.R., Kumawat, M.K., Singh, U.P. (2014). Structure-guided discovery of 1,3,5-triazine-pyrazole conjugates as antibacterial and antibiofilm agent against pathogens causing human diseases with favorable metabolic fate. *Bioorganic Med. Chem. Lett.* 24, 3321- 3325. doi: 10.1016/j.bmcl.2014.05.103.

Singh, U.P., Pathak, M., Dubey, V., Bhat, H.R., Gahtori, P., Singh, R.K. (2012). Design,

Accepted Article
synthesis, antibacterial activity, and molecular docking studies of novel hybrid 1,3-thiazine-1,3,5-triazine derivatives as potential bacterial translation inhibitor. *Chem. Biol. Drug Des.* 80, 572- 583. doi: 10.1111/j.1747-0285.2012.01430.x.

Srivastava, J.K., Awatade, N.T., Bhat, H.R., Kmit, A., Mendes, K., Ramos, M., Amaral, M.D., Singh, U.P. (2015). Pharmacological evaluation of hybrid thiazolidin-4-one-1,3,5-triazines for NF- κ B, biofilm and CFTR activity. *RSC Adv.*, 5, 88710–88718. doi: 10.1039/C5RA09250G.

Truelsen, T., Begg, S., Mathers, C.D., Satoh, T. (2000). Global burden of cerebrovascular disease in the year 2000. Global burden of disease 2000 working paper. Geneva, World Health Organization, 2000 (http://www.who.int/healthinfo/statistics/bod_cerebrovasculardisease.pdf, accessed 6 June 2008).

Unterberg, A.W., Stover, J., Kress, B., Kiening, K.L. (2004). Edema and brain trauma. *Neuroscience*, 129, 1021-1029. DOI: 10.1016/j.neuroscience.2004.06.046

Vazzana, I., Terranova, E., Mattioli, F., Sparatore, F. (2004). Aromatic Schiff bases and 2,3-disubstituted-1,3-thiazolidin-4-one derivatives as antiinflammatory agents. *Arkivoc*, 5, 364-374.

Vembu, S., Pazhamalai, S., Gopalakrishnan, M. (2016). Synthesis, spectral characterization, and effective antifungal evaluation of 1H-tetrazole containing 1,3,5-triazine dendrimers. *Med. Chem. Res.* 25, 1916-1924. doi: 10.1007/s00044-016-1627-6

Vicini, P., Geronikaki, A., Anastasia, K., Incerti, M., Zani, F. (2006). Synthesis and antimicrobial activity of novel 2-thiazolylimino-5-arylidene-4-thiazolidinones. *Bioorganic Med. Chem.* 14, 3859-3864. doi: 10.1016/j.bmc.2006.01.043

Werner, C., Engelhard, K. (2007). Pathophysiology of traumatic brain injury. *Br. J. Anaesth.* 99, 4–9. DOI: 10.1093/bja/aem131

Zacharie, B., Abbott, S.D., Duceppe, J.S., Gagnon, L., Grouix, B., Geerts, L., Gervais, L., Sarra-Bournet, F., Perron, V., Wilb, N., Penney, C.L., Laurin, P. (2018). Design and Synthesis of New 1,3,5-Trisubstituted Triazines for the Treatment of Cancer and Inflammation. *ChemistryOpen*, 7, 737- 749. doi: 10.1002/open.201800136.

Zhang, W., Potrovita, I., Tarabin, V., Herrmann, O., Beer, V., Weih, F., Schneider, A.,
Schwaninger, M. (2005). Neuronal activation of NF-kappaB contributes to cell death in
cerebral ischemia. *J Cereb Blood Flow Metab.*, 25(1), 30-40. doi:
10.1038/sj.jcbfm.9600004

Figure captions

Scheme 1: Synthesis of target compounds 8(a-n). Where a) various amines, stirring, aq. NaOH, 0–5 °C, b) morpholine, reflux, aq. NaOH 40–55 °C; (b) NH₃, reflux, 125–135 °C; (c) toluene, reflux, 110 °C.

Figure 1: Effect of compound 8k on (a) neurological deficit score and (b) cerebral edema percentage. Values represent the mean ± SD and are representative of three independent experiments. ##P < 0.05 vs sham; **P < 0.01 vs. MCAO, one-way analysis of variance followed by a Tukey's *post hoc* test.

Figure 2: Effect of 8k on the histopathology of brain coronal section.

Figure 3: Effect of compound 8k on the brain infarct area of MCAO mice. Values represent the mean ± SD and are representative of three independent experiments. ##P < 0.05 vs sham; **P < 0.01 vs. MCAO, one-way analysis of variance followed by a Tukey's *post hoc* test.

Figure 4: Effect of compound 8k on pro-inflammatory mediators (a) TNF- α , (b) IL- β and (c) IL-6. Values represent the mean \pm SD and are representative of three independent experiments. $^{##}P < 0.05$ vs sham; $^{**}P < 0.01$ vs. MCAO, one-way analysis of variance followed by a Tukey's *post hoc* test.

Figure 5: Effect of compound 8k on the oxidative stress in the MCAO mice (a) MDA, (b) SOD and c) GSH. Values represent the mean \pm SD and are representative of three independent experiments. $^{##}P < 0.05$ vs sham; $^{**}P < 0.01$ vs. MCAO, one-way analysis of variance followed by a Tukey's *post hoc* test.

Figure 6: Effect on the apoptosis related genes. (a) cleaved caspase-3, (b) Bax and (c) Bcl-2. Values represent the mean \pm SD and are representative of three independent experiments. $^{##}P < 0.05$ vs sham; $^{**}P < 0.01$ vs. MCAO, one-way analysis of variance followed by a Tukey's *post hoc* test.

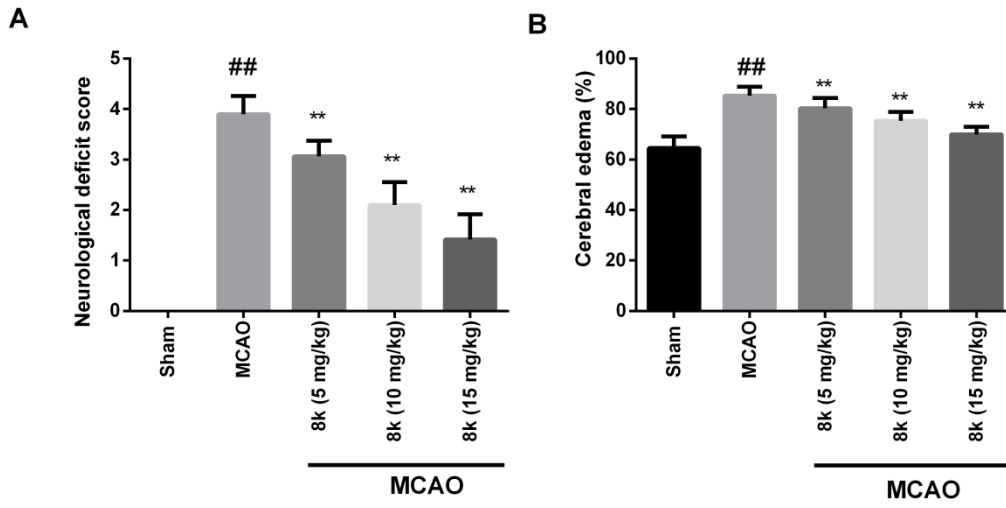
Figure 7: Effect on Nf- κ B signalling pathway. (a) p-I κ B α and (b) NF- κ B. Values represent the mean \pm SD and are representative of three independent experiments. $^{##}P < 0.05$ vs sham; $^{**}P < 0.01$ vs. MCAO, one-way analysis of variance followed by a Tukey's *post hoc* test.

List of Tables

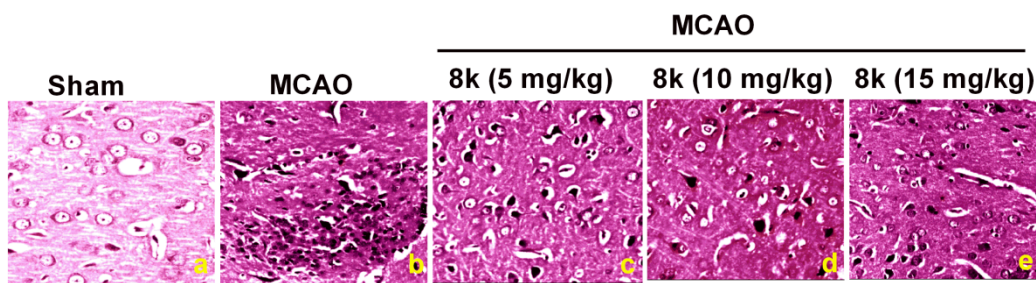
Table 1: Inhibitory activity of compounds (**8a-n**) on NF- κ B transcriptional activity in LPS-stimulated RAW264.7 cells.^a

Entry	R ₁	R ₂	IC ₅₀ (in μ M) ^a
8a	H	4-Cl	> 100
8b	4-Cl		22.12 \pm 5.67
8c	4-F		19.23 \pm 2.11
8d	4-NO ₂		15.65 \pm 1.92
8e	4-OH		31.36 \pm 3.72
8f	4-OCH ₃		49.56 \pm 4.73
8g	4-CH ₃		> 100
8h	H	4-F	10.34 \pm 0.86
8i	4-Cl		3.33 \pm 0.23
8j	4-F		4.21 \pm 0.67
8k	4-NO ₂		0.90 \pm 0.12
8l	4-OH		5.89 \pm 1.14
8m	4-OCH ₃		10.11 \pm 2.33
8n	4-CH ₃		7.34 \pm 1.50
Dexamethasone (Reference)			0.95 \pm 0.56

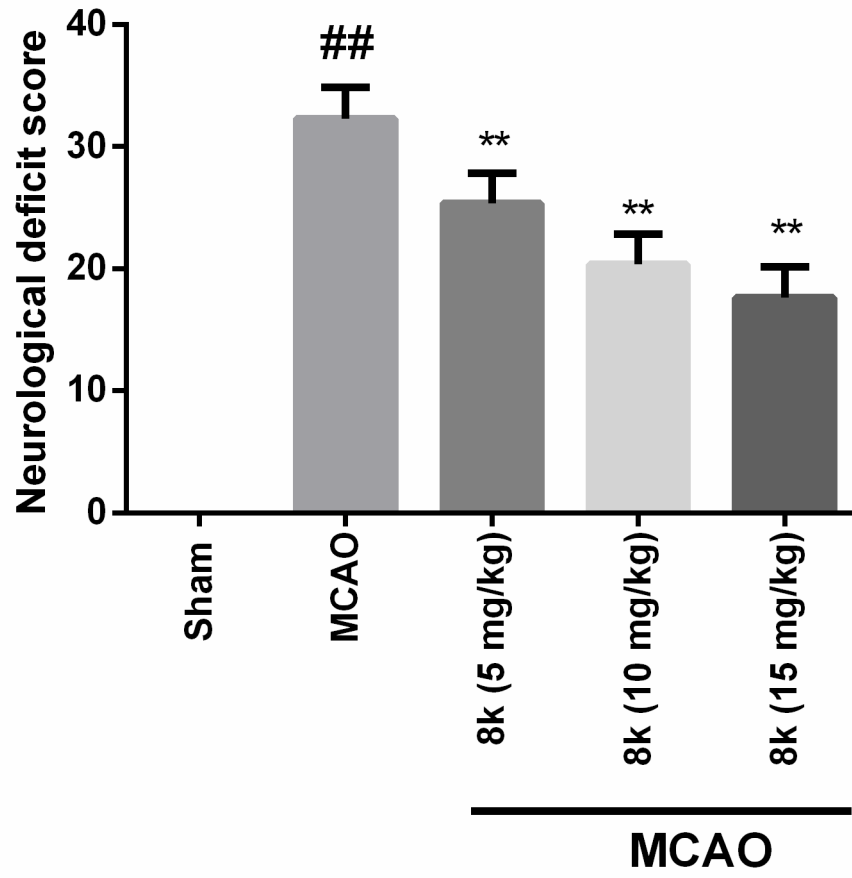
^a IC₅₀ values expressed as mean \pm SD of at least three independent assays, ** P < 0.01 vs. Control, ## P < 0.01 vs. LPS



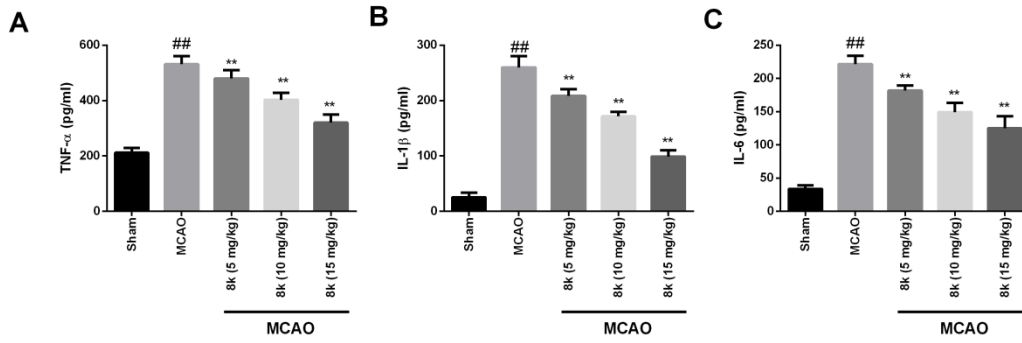
cbdd_13744_f1.tif



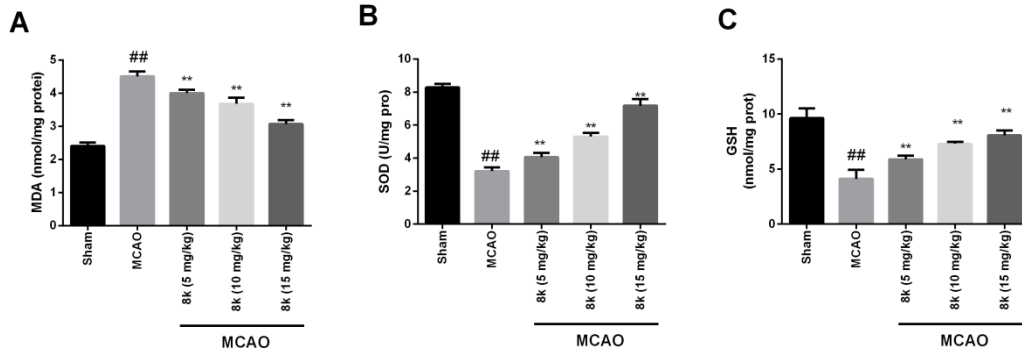
cbdd_13744_f2.tif



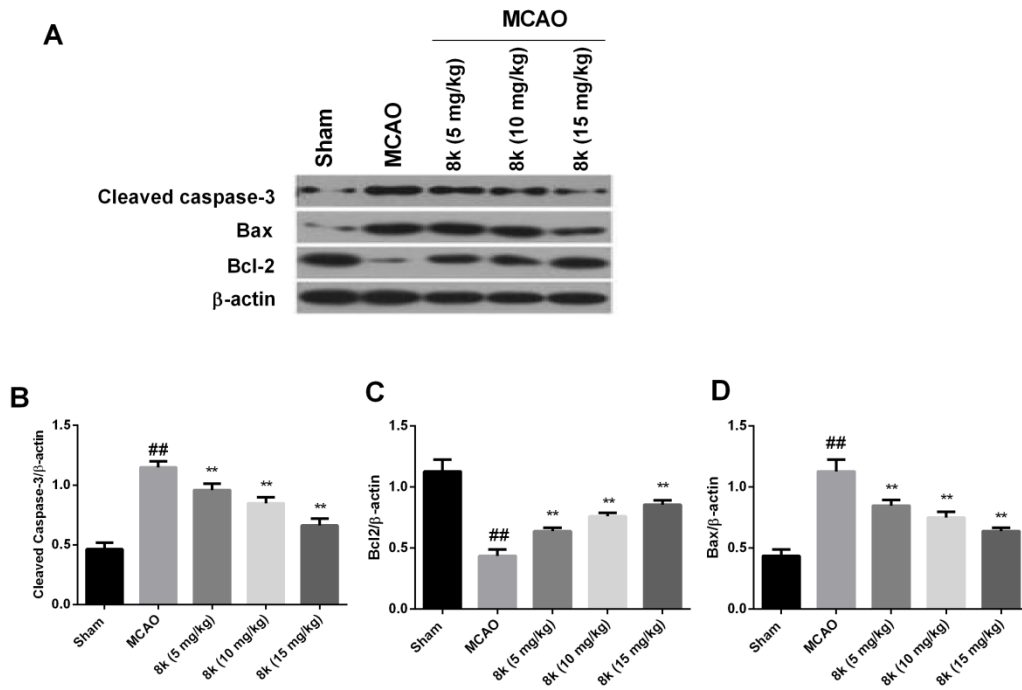
cbdd_13744_f3.tif



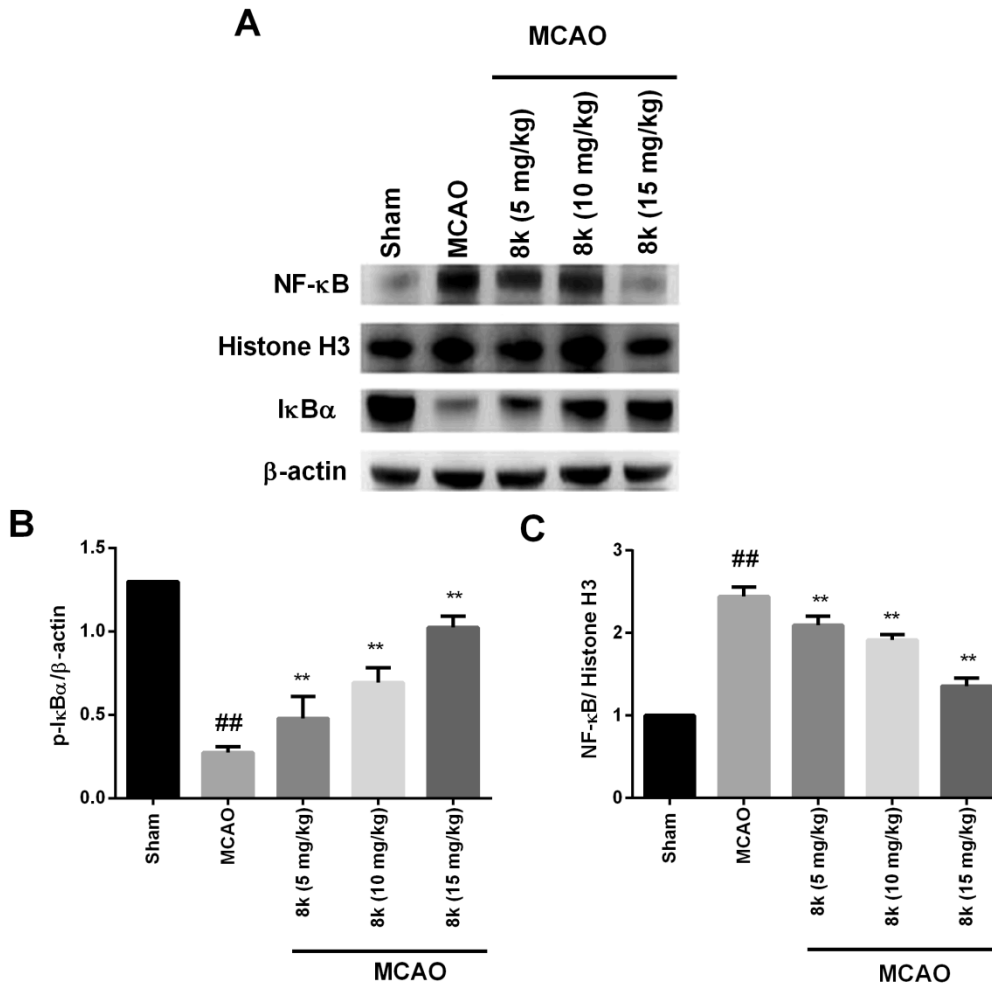
cbdd_13744_f4.tif



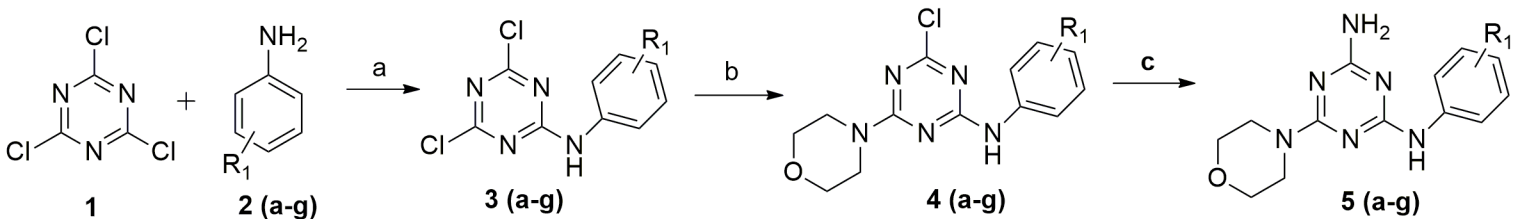
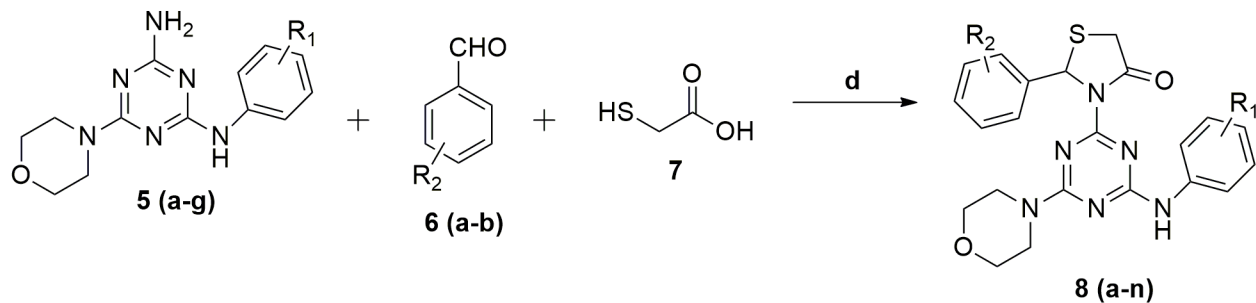
cbdd_13744_f5.tif



cbdd_13744_f6.tif



cbdd_13744_f7.tif

Step 1**Step 2**

Entry	R ₁	R ₂
8a	H	
8b	4-Cl	
8c	4-F	
8d	4-NO ₂	4-Cl
8e	4-OH	
8f	4-OCH ₃	
8g	4-CH ₃	

Entry	R ₁	R ₂
8h	H	
8i	4-Cl	
8j	4-F	
8k	4-NO ₂	4-F
8l	4-OH	
8m	4-OCH ₃	
8n	4-CH ₃	